Supporting Information

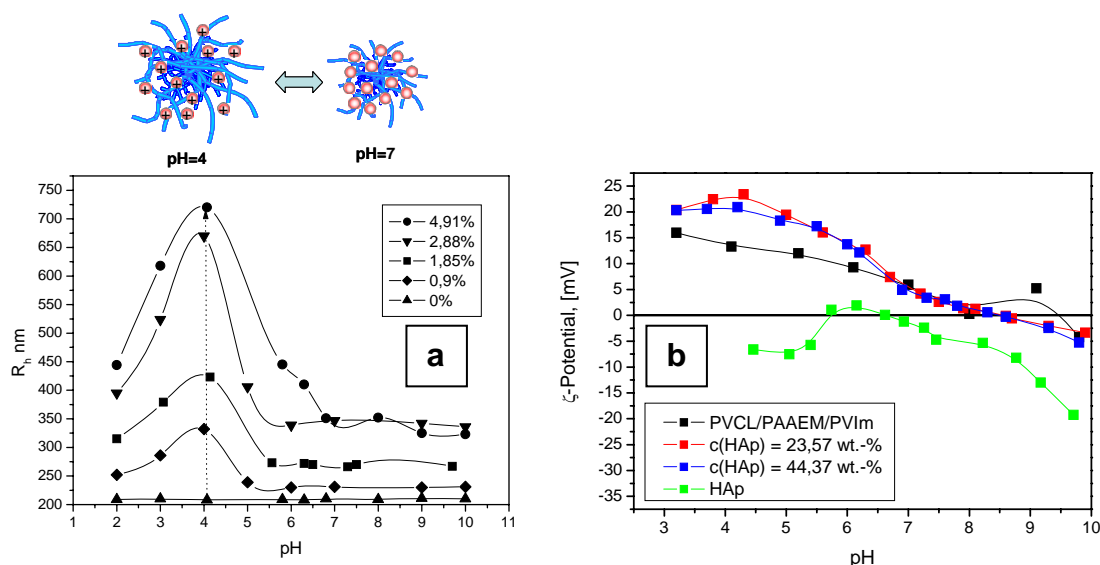# Aqueous Microgels for Growth of Hydroxyapatite Nanocrystals

Susann Schachschal, Andrij Pich*, Hans-Juergen Adler

Colloidal properties of microgels

Fig. S1a shows the hydrodynamic radii of different microgel samples as a function of pH (light scattering data). The R_h – pH dependencies for all samples containing VIm exhibit maximum at pH=4 what correlates with maximum ionization pH of VIm units. This effect leads to the swelling of microgel particles due to the strong electrostatic repulsion between the charged VIm groups. Fig. S1a indicates also that the swelling at pH=4 increases gradually with increase of the VIm content in the microgel structure indicating that the repulsion forces within the microgel particle became stronger at higher concentration of charged VIm groups. The decrease of the R_h values at pH>4 is attributed to the increase of the ionic strength by excess of HCl and screening of the electrostatic repulsion within microgel particles. By performing the measurement at constant ionic strength (using buffer solution for the adjustment of the pH-value) one can avoid such effect and R_h values should remain constant at pH<4. Contrary, the hydrodynamic radius of VCL/AAEM microgels is not influenced by the pH indicating that microgels do not contain ionizable groups. The experimental results presented in Fig. S1a demonstrate that by incorporation of small amounts of VIm groups into VCL/AAEM microgels it is possible to prepare highly pH-sensitive particles and the maximum swelling degree can be easily controlled by the amount of ionizable groups in the polymer network.

The electrophoretic mobility measurements (Fig. S1b) indicate that microgels are positively charged in acidic pH and possess a weak charge at neutral and basic pH. This correlates with DLS data presented above. The composites with deposited HAp exhibit similar behaviour to original microgels. This indicates that HAp nanocrystals incorporated into microgels do not contribute to the surface charge.
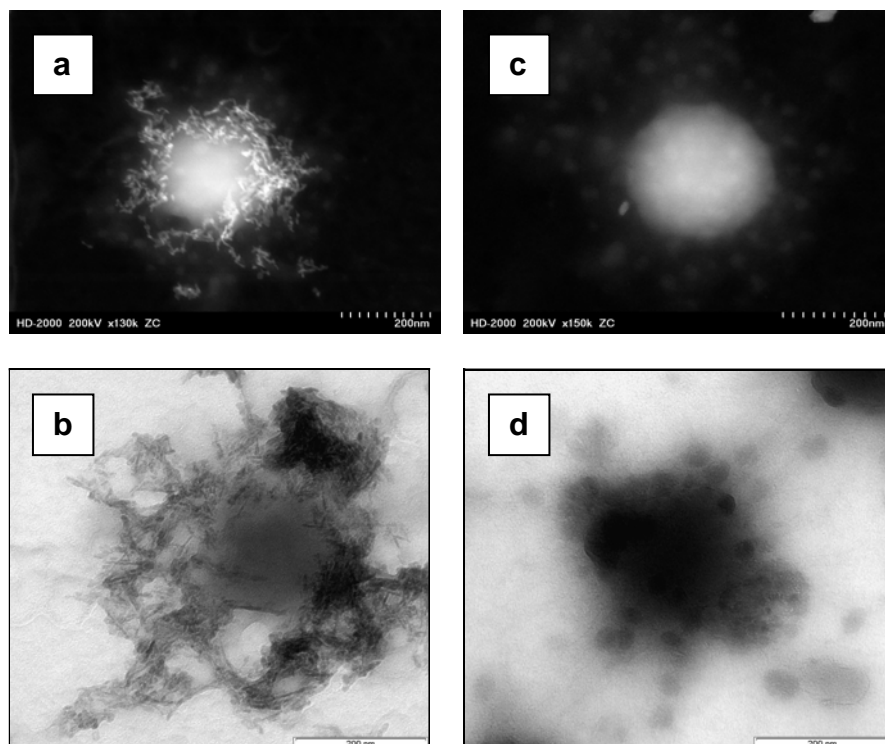

Figure S1. pH-dependency of hydrodynamic radii for microgels with different VIm content (T=20°C) (a); Z-potential as a function of pH (b).

HAp deposition

The control experiment was performed to check if Ca-ions can be entrapped by microgel network. The microgel and calcium nitrate solution were mixed together and after 12 hours we have dialysed the sample to remove "free" Ca-ions. After 3 days dialysis we used purified sample and performed synthesis of HAp (by adding ammonium phosphate and adjusting pH to 9). As reference another experiment has been carried out where loading of the HAp was performed in similar conditions but no dialysis step has been conducted.

The results were following. The dialysed sample showed content of the inorganic phase around 7 wt.-% and non-dialysed sample contained 44 wt.-% of HAp. Obviously, the large amount of Ca-ions has been removed from the microgel dispersion. However, some fraction of metal ions was entrapped by microgel network and further transformed to calcium phosphate.
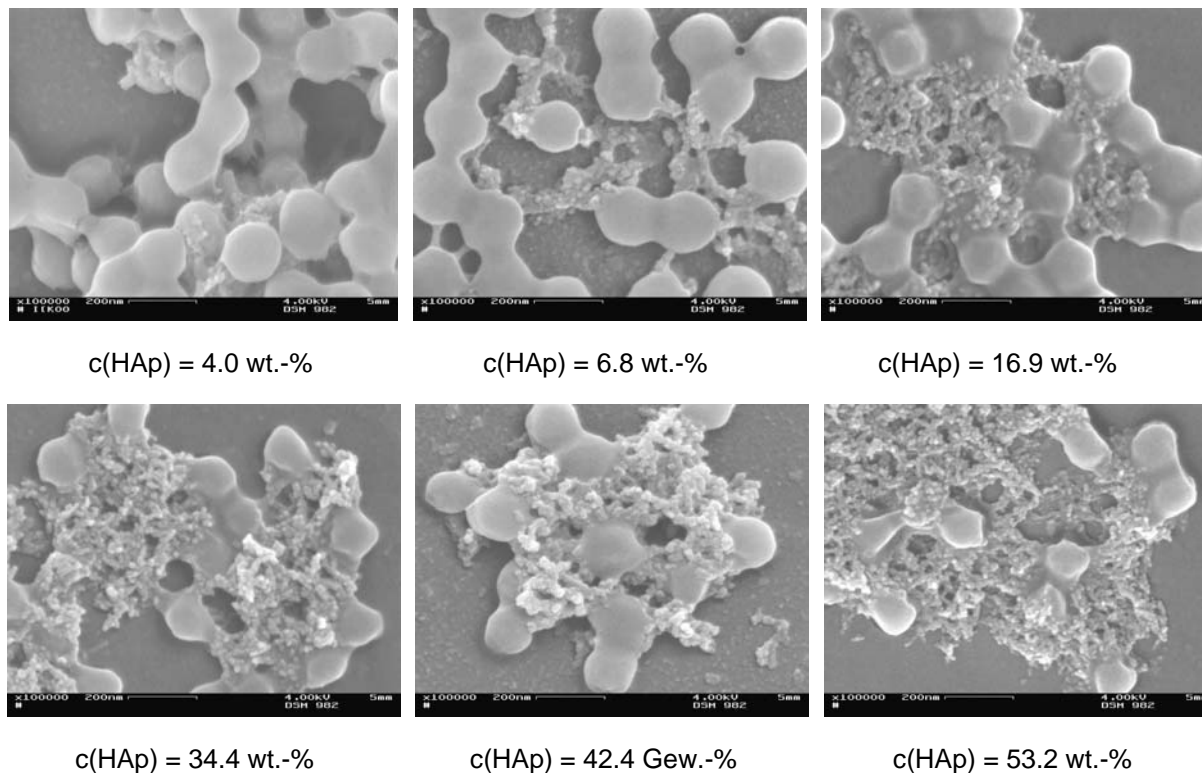

Figure S2. Dark-field STEM (top) and bright-field TEM (bottom) images of microgel particles containing 44.34 wt.-% (a,b) and 7.06 wt.-% (c,d) HAp nanocrystals.
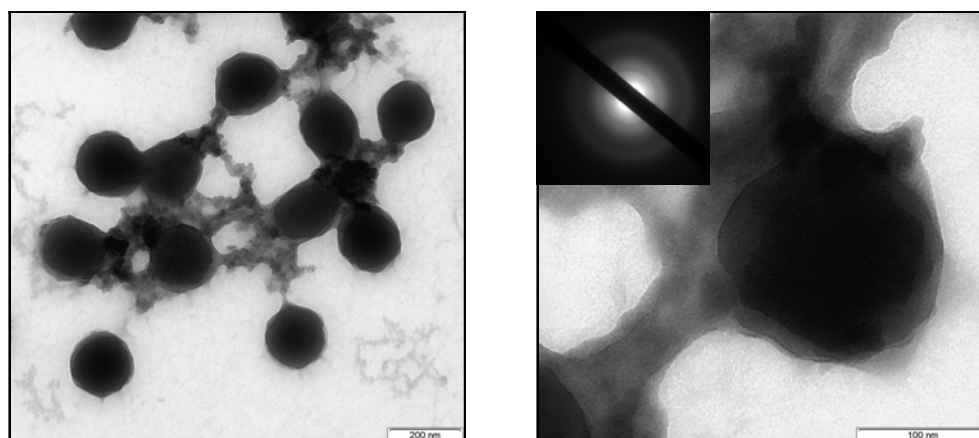
It is interesting to note that the morphology of the formed HAp is quite different in two cases (Fig. S2). The sample prepared in "conventional way" exhibits needle-like HAp nanocrystals. In the case of dialysed sample we can see small spherical amorphous particles that tend to form larger domains. Probably the formation of crystalline HAp nanorods is hindered in the situation when in the reaction system only "immobilized" Ca-ions are available. This may lead to the conclusion that "free" Ca ions are necessary to support the crystal growth within microgel.
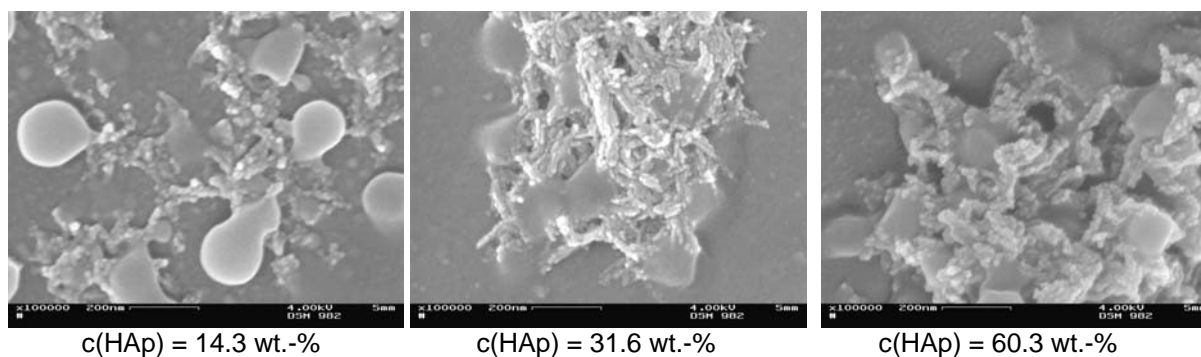
Morphology of hybrid microgels

The deposition of HAp has been performed in VCL/AAEM microgels (no N-vinylimidazole groups) and VCL/AAEM/DMAPMAm microgels (instead of N-vinylimidazole *N*-[3-(diethylamino)propyl] methacrylamide was used) to study the importance of functional groups in the microgel structure for the deposition of HAp.
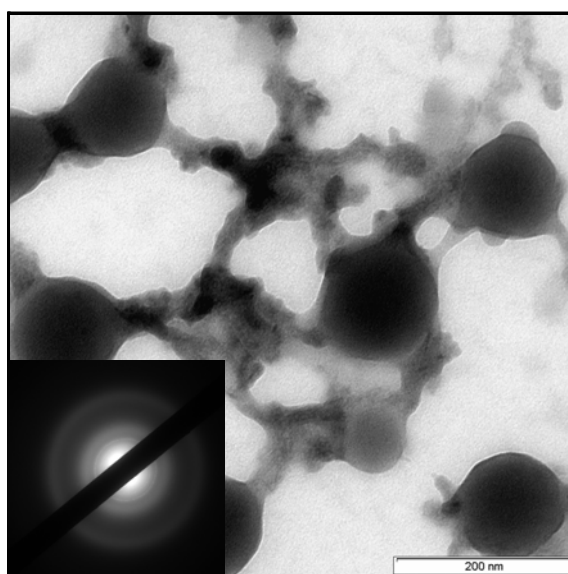

| c(HAp) = 4.0 wt.-% | c(HAp) = 6.8 wt.-% | c(HAp) = 16.9 wt.-% |

| c(HAp) = 34.4 wt.-% | c(HAp) = 42.4 Gew.-% | c(HAp) = 53.2 wt.-% |

Figure S3. SEM images of VCL/AAEM/HAp composites.

Figure S4. TEM images of VCL/AAEM/HAp composites (16.9% HAp).

c(HAp) = 14.3 wt.-%   c(HAp) = 31.6 wt.-%   c(HAp) = 60.3 wt.-%

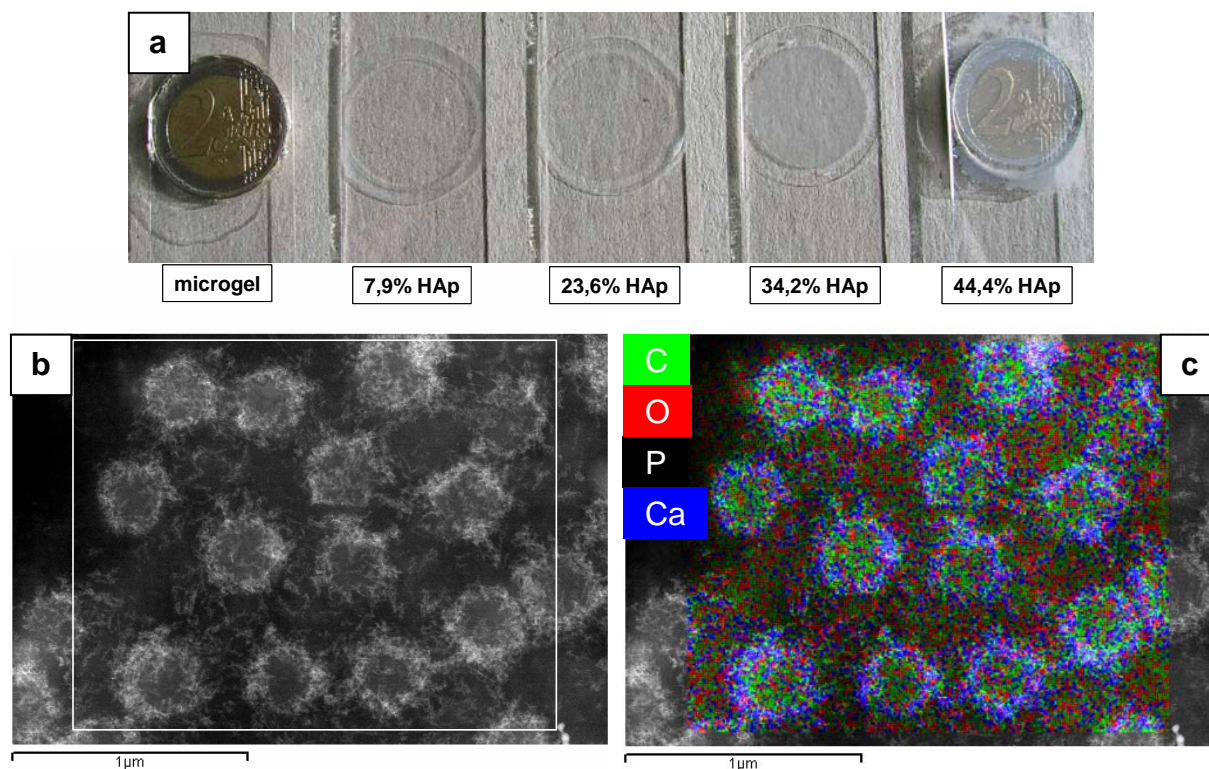**Figure S5.** SEM images of VCL/AAEM/DMAPMAm/HAp composites.

Figure S6. TEM images of VCL/AAEM/DMAPMAm/HAp composites (16.9% HAp).

The microscopy images presented in Fig. S3-S6 indicate that VCL/AAEM and VCL/AAEM/DMAPMAm microgel systems are not suitable for the controlled deposition of HAp nanocrystals. The microscopy images indicate that HAp is formed on the surface of the microgels or directly in aqueous phase leading to the formation of interparticle bridges and leading to the coagulation of the colloids. This results indicate a positive influence of the vinylimidazole groups for the controlled growth of HAp nanocrystals in the microgel network.

Composite films

The thin films have been prepared by drying of hybrid microgel dispersion on the glass support. Water has been removed by evaporation at room temperature. The average film thickness in dry state was 5 μm. Fig. S7a shows photographs of dried microgel films on glass substrates. Even at high HAp loading films remain transparent what indicates that no strong phase separation occurs during drying process. Fig. S7b shows TEM image of the thin fragment of the microgel film that proves additionally that HAp NCs remain embedded into polymeric network and no migration of the inorganic component occurs. The white line in Fig. S7b shows the area used for the EDX mapping to determine the element distribution. Fig. S7c indicates that the strongest Ca signal is detected around microgel core, so the composite structure of the microgel is preserved after film-formation.

Figure S7. Photograph of films prepared from VCL/AAEM/VIm-HAp hybrid microgels (a); TEM image of the composite film fragment obtained by drying VCL/AAEM/VIm-HAp (52.2%) sample (b); EDX element mapping showing distribution of different elements (c).